MRS Advances
https://doi.org/10.1557/s43580-025-01233-8

ORIGINAL PAPER

Multifunctional CVD diamond window for Infrared imaging

Raphaël Guillemet[1] · Mane-Si Laure Lee[1] · Doriane Jussey[1] · Elyess Traouli[1] · Brigitte Loiseaux[1] · Patrick Garabédian[1] · Sirine Ben Khemis[2] · Emmanuel Scorsone[2] · Edoardo Rossi[3] · Saqib Rashid[3] · Marco Sebastiani[3]

Received: 22 November 2024 / Accepted: 4 March 2025

Abstract
Diamond is well known for its outstanding thermal, electrical, and mechanical properties, but is also of great interest for optical and imaging applications. Imaging systems offer increasing performances, with high functionalities and technicity, but are often exposed to harsh or visually degraded environments. In this paper, we exploit some of the multiple physical properties of chemical vapor deposition (CVD) diamond and demonstrate the feasibility of diamond-based metasurface multifunctional windows for infrared spectral range, throughout different configurations. The resulting 2″ full diamond optical window provides imaging systems with several functionalities, including antireflective optical properties with an enhanced transmission up to 80–90% in the 8–14 µm spectral range, high mechanical resistance, superhydrophobicity, antirain, and antimist behaviors. Moreover, the electrochemical activation of a boron-doped diamond-based window leads to self-cleaning properties, thus paving the way for the imaging system to low maintenance operations and 24/7 operation.

Introduction

Optronics systems are based on increasing technicality in order to achieve better performances, but they are often subjected to harsh operational or environmental conditions. Optronics equipment is usually protected by windows, especially in the case of outdoor surveillance systems, which need to operate in any environmental conditions, including wet or rainy conditions. In maritime surveillance for instance, the camera's windows must be equipped with wipers that require regular, expensive, and complex maintenance. Avoiding wipers by proposing multifunctional windows offering both antireflection and superhydrophobicity is thus of interest.

Optronics systems may also encounter visually degraded conditions, caused by either dust, sand, oil, or fuel contamination, which can also degrade the quality of the image and prevent their 24/7 full operation.

The results of many studies have been published in the field of bio-inspired structures for superhydrophobicity or multifunctional superhydrophobic/antireflective properties. Among them, we can find applications in the visible [1, 2] and near-infrared [3] spectral regions on fused silica substrate or glass. In the infrared, studies on germanium or silicon were reported for applications in the LongWave InfraRed (LWIR) or MidWave InfraRed (MWIR) [4–6] showing their benefit both at laboratory level and on functional imaging product devices. Antimist behavior of structured surfaces was also demonstrated for specific geometries of structures [7].

Diamond is well known for its outstanding thermal, electrical, and mechanical properties, but is also of great interest for optical applications: It is well suited for broadband applications of multi-band operation due to its good optical transmission over a large spectral range from visible to LWIR 400 nm-15 µm. With the progress of the nanotechnologies, diamond can also be structured at a subwavelength scale, *i.e.,* at a scale that is much smaller than the operation wavelength, enabling the synthesis of an artificial material characterized by an effective index [8]. By controlling locally the shape and the size of the structures along the *z*-direction, a gradient effective index, avoiding reflection at the interface

✉ Raphaël Guillemet
raphael.guillemet@thalesgroup.com

1 Thales Research & Technology, Campus Polytechnique, 1 Avenue Augustin Fresnel, 91767 Palaiseau, France

2 Diamond Sensors Laboratory, CEA, LIST, 91191 Gif-Sur-Yvette, France

3 Department of Civil, Computer Science and Aeronautical Technologies, Università Degli Studi Roma Tre, Via Vito Volterra 62, 00146 Rome, Italy

Published online: 18 March 2025

substrate/air and acting as an antireflective coating, can be synthesized [9–15] (Fig. 1a, b).

In this paper, we aim to demonstrate that CVD diamond may enable multifunctional windows to provide antireflective, superhydrophobic, antirain, and antimist properties with high mechanical resistance and antifouling behavior for optronics imaging systems.

Methods and results

Manufacturing of LWIR metasurfaces windows

A CVD diamond window was purchased at Coherent Corp. (diameter of 2'', thickness of 1 mm, and average roughness < 15 nm on both faces). A technological process was developed to get ~ 2 µm periodic conical structures with an aspect ratio higher than 1:4. The manufacturing of the window is based on the process flow described in Fig. 1c. It consists of a lithography step enabling the definition of the patterns in a resist layer then transferred in a Ni-based metallic mask deposited by sputtering, and followed by a RIE-ICP (Reactive Ion Etching – Inductively Coupled Plasma) using O_2 plasma etching step, hence enabling high aspect ratio microstructuration of the diamond substrate. An additional chemical functionalization step is carried out leading to superhydrophobicity. Note that the lithographic step is based on the well-known nano-imprint lithography, which is a scalable process also compatible with curved surfaces.

Figure 1d shows a picture of the 2″ multifunctional diamond window and Scanning Electron Microscopy (SEM) images of different shapes of the structures that can be achieved by adjusting the etching process.

Antireflective optical properties

In terms of optical performances, the main target is a transmission higher than 90% per surface in the LWIR spectral band (representing approximately 81% for a two-sided structured window).

The achieved double-sided transmission is measured by FTIR (Fourier-Transform Infrared Spectroscopy) at normal incidence. As shown in Fig. 2a, transmission for the whole window in between 80 and 90% is achieved in the [8 µm-14 µm] range, as compared to ~ 68% transmission in the case of flat polished diamond, showing a transmission increase of ~ 20% to 30% (blue line). As a matter of comparison, we have computed, with Rigorous Coupled Wave Analysis (RCWA), the transmission of the window, considering the manufactured geometries and assuming no multiple reflections in the window substrate (see dashed green line). The enhancement in terms of transmission is significant for imaging systems as it results into a gain in terms of sensitivity.

Fluidic properties

The wettability of the nanopatterned surface was assessed by measuring the drop contact angle, using the Drop Shape Analyzer-DSA 100 from Krüss. After functionalization of the surface with a few nm thick polytetrafluoroethylene (PTFE) layer obtained by a C_4F_8 plasma, inducing no absorption in LWIR range, a contact angle of ~ 160° was measured with DI or tap water, demonstrating the superhydrophobic behavior. Note that this measurement was performed few minutes after the surface functionalization. However, no change in terms of contact angle has been observed more than one year later.

In order to assess the antirain property of the window, the latter was implemented in front of an uncooled camera (pixel size of 25 µm) equipped with an optical lens (*f* number of 1.3 and focal length of 18 mm) operating in LWIR (8–12 µm). The images in Fig. 2b-left and right were taken with a standard non-coated germanium window and with the multifunctional window, respectively. During water spraying, the images of Fig. 2b-bottom illustrate that with the multifunctional window, water droplets does not stick at the surface of the window but bounce; hence, no degradation of the image quality is observed. In contrast, in the case of the germanium window, the droplets remain stuck at the surface of the window, resulting into a blur effect reducing significantly the image quality. These pictures assess the benefit of the multifunctional window for LWIR imaging in terms of image quality improvement under degraded environment.

The multifunctional window was also tested against mist. The experiment consisted in an in situ optical microscope observation of the multifunctional window, compared to standard germanium window, during mist growth at 5 °C. Figure 2c illustrates pictures taken during the mist growth at different time. While the standard window is almost totally covered in the observed region after 180 s, we can observe, for the multifunctional windows, the coalescence of the microdroplets resulting in their ejection, hence limiting the accumulation of mist.

Mechanical resistance

Diamond-like carbon (DLC) coating is well known to increase the mechanical resistance of optical components and to protect metasurfaces made of conventional soft materials, like germanium [16]. However, its hardness is lower than that of diamond (10–80 GPa *VS* 100 GPa for diamond), and DLC could be an inefficient hard coating for harsh environments.

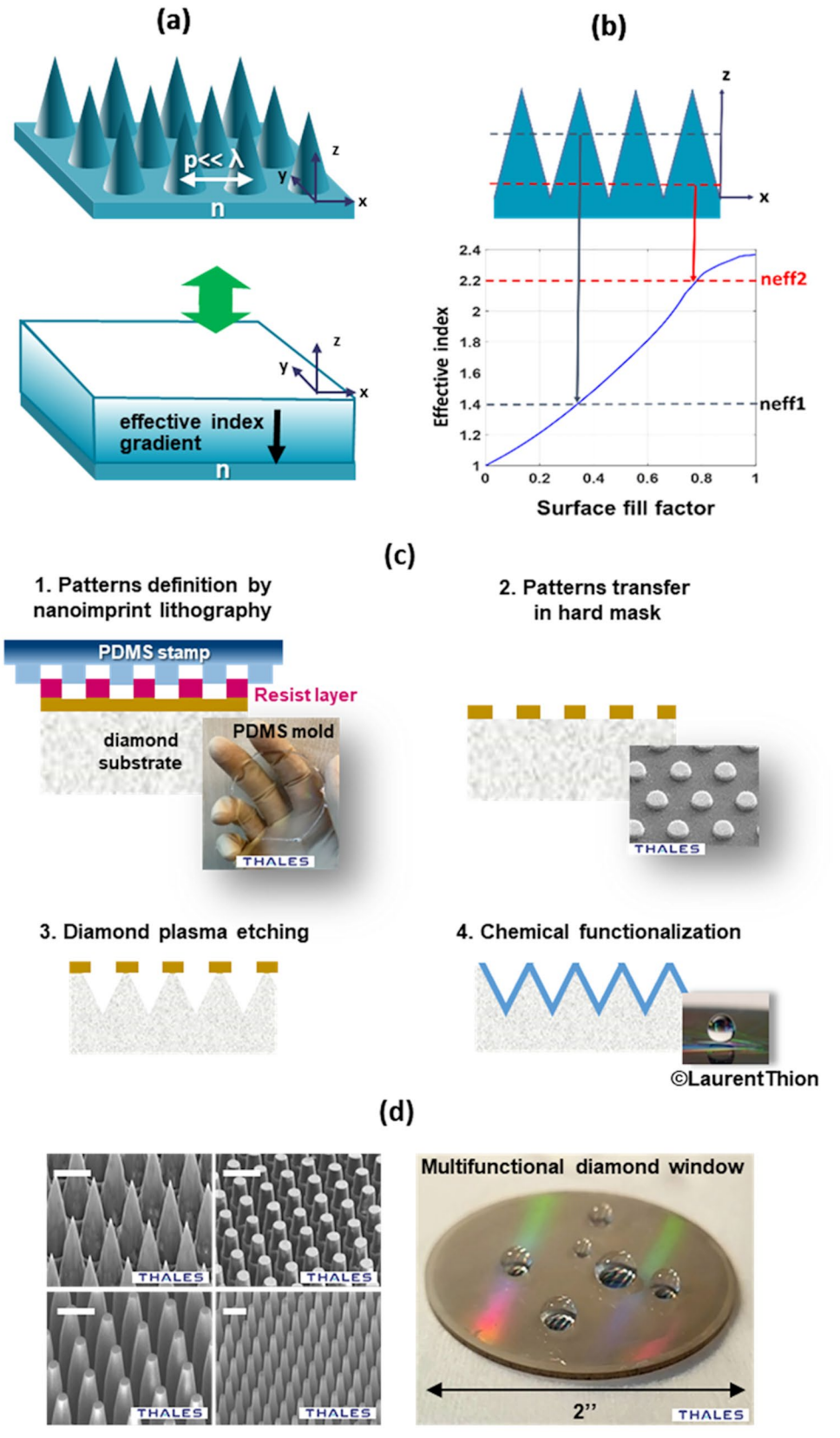

Fig. 1 **a** Simplified schematics for artificial material representing subwavelength periodic structures of period p much smaller than the wavelength and its simplified artificial material representation. **b** Local effective index as a function of the surface fill factor, enabling effective index gradient synthesis along the z-axis to provide index adaptation between air and substrate. **c** Main process flow followed for the manufacturing of the 2'' diamond multifunctional window (**d**), and examples of several structures geometries that can be obtained by etching process tuning. The scale bar on the SEM images is 2 µm

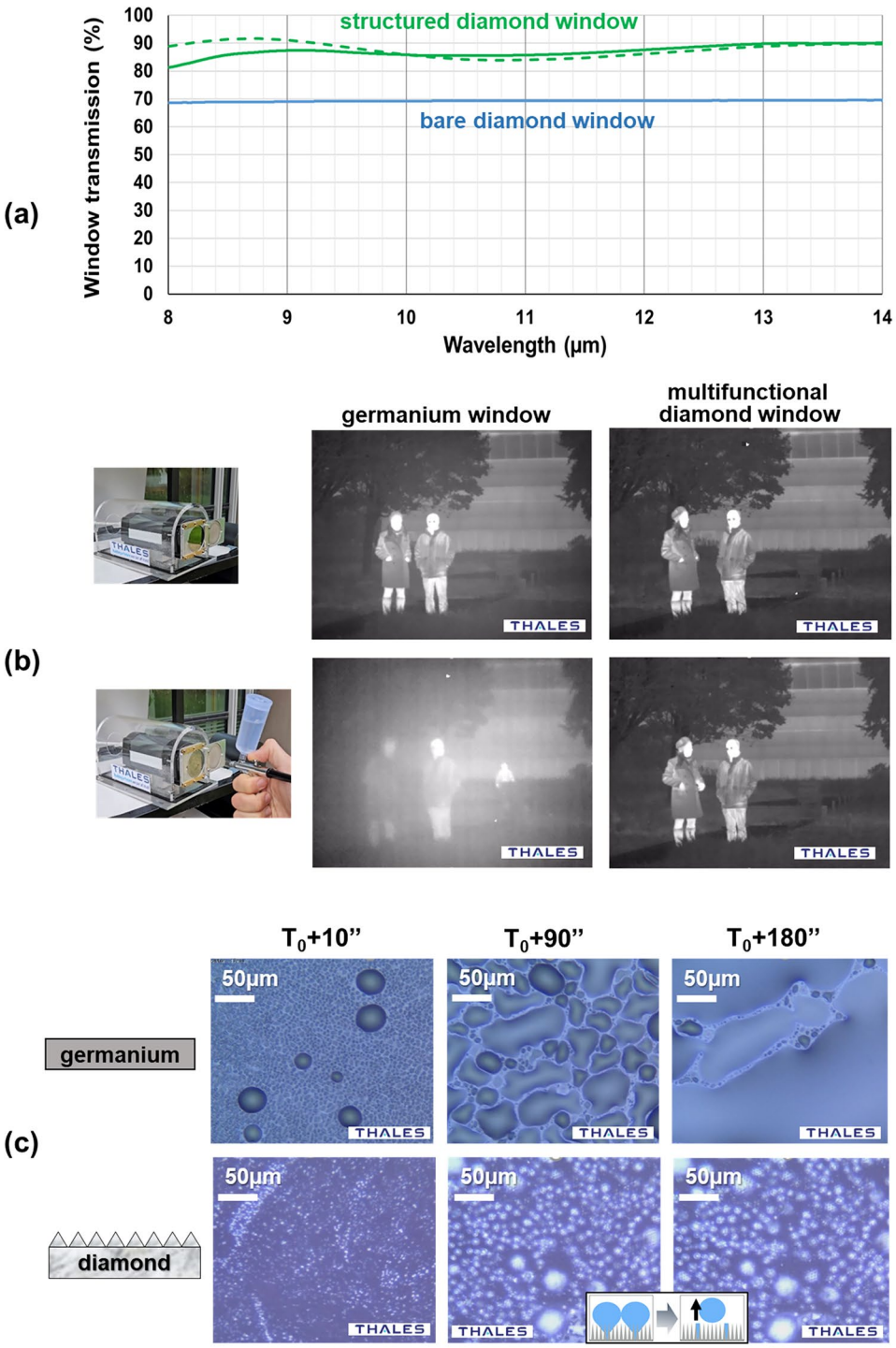

Fig. 2 **a** Optical transmission of a structured CVD diamond window (green line), as compared to the bare surface (blue line). The window is structured on both faces. Comparison with theoretical transmission considering the manufactured profile (dashed green line), assuming no multiple reflections. **b** Images from a LWIR uncooled camera in presence of water, with a standard germanium window (left) and with the multifunctional CVD diamond window (right), before (top) and during water spraying (bottom). **c** Optical microscope pictures taken during mist growth on a standard germanium window (top) and the multifunctional window (bottom)

Here, we evaluate the resistance of diamond-based microstructured windows by nanoscratch. Nanoscratch testing leverages the advantages of nanoindentation, particularly in terms of small probing volumes and the ability to record both vertical (F_n) and lateral/transverse loads (F_t), as well as related displacements during testing. Nanoindentation is a well-known technique for testing the mechanical properties of materials on small scales, where the principle involves pressing a hard tip, often made from a highly durable material like diamond, into a sample with unknown properties to derive its mechanical characteristics. Nanoscratch testing employs this principle while simultaneously moving the stage to perform a controlled scratching motion, continuously recording the material's response, including displacement and forces. This allows for the measurement of both the vertical force and the lateral force, which is especially

valuable for determining the coefficient of friction and assessing surface mechanical behavior.

In the context of nanoscratch testing, the mechanical resistance of diamond structures on a silicon substrate was compared to germanium structures coated with DLC or with CVD diamond. For consistent comparison, both the period and height of the structures were maintained approximately at same values, 1.5 µm and 5 µm, respectively.

Nanoscratch tests were conducted using a G200 nanoindenter from KLA Corp., equipped with a sphero-conical diamond tip with a 52 µm radius. Prior to testing, the area function of this tip was calibrated on a reference fused quartz sample. This calibration step also ensured that the frame stiffness was adequately calibrated and corrected, which is particularly critical given the stiff nature of the diamond structures being tested. Accurate calibration of the frame stiffness is essential for reliable force–displacement data during nanoscratch testing. For all samples, the starting setpoint of the vertical force for nanoscratching was 1 mN. This force produced distinct behaviors in the DLC-coated and diamond-coated germanium samples, as shown in Fig. 3a. Specifically, DLC-coated germanium nanostructures were observed to break at mid-height, while diamond-coated germanium exhibited erosion only at the top of the structures. In contrast, for full diamond structures, no visible breakage was noticed under the same 1 mN vertical loading, as confirmed through SEM analysis. To further investigate and compare these behaviors, the vertical loading was increased to 5 mN. Even at this increased load, Fig. 3a demonstrates that the full diamond structures only showed blunting at the very top of the nanostructures, potentially due to localized crystal plasticity phenomena arising from high-contact pressures at the tip.

While variations in apex curvature across the samples may exist, the early failure of the germanium-coated structures is still primarily driven by the intrinsic brittleness of germanium. In the case of full diamond structures, even when using a sharper tip geometry that precisely follows the geometry of the germanium-coated samples, the observed behavior still predominantly involves crystal plasticity phenomena at the contact points. This further confirms that full diamond structures are highly resistant to scratch-induced breakage.

Since this study relies on nanoscratch testing for a comparative failure mode analysis rather than deriving absolute mechanical properties, the applied load remains valid regardless of potential tip wear. AFM measurements confirm that damage was limited to the tip in use, ensuring the reliability of the observed failure mechanisms. To verify the absence of substantial tip wear, we performed AFM characterizations before and after three scratches under the same conditions on the employed sphero-conical tip (at the very top of the tip itself). To isolate the tip's intrinsic roughness from its geometrical shape, we applied a spherical fitting process as shown in Fig. 3b, c. The convoluted radius before and after testing was 40.6 µm ± 22.0 nm and 39.0 µm ± 14.6 nm, respectively, with no meaningful difference, indicating the tip curvature remained unchanged ;hence, confirming that damage was limited to the tip in use, ensuring the reliability of the observed failure mechanisms.

Abrasion tests according to standard NFS10-005–4 / NF ISO 9211–4, considering a degree of severity 4/4 (*i.e.,* 40 frictions @10N), were carried out on diamond structures grown on a silicon substrate. The SEM analysis shows a geometry of structures that is still intact with no observed breakage. Note that cheesecloth residues are nestled between the structures (see Fig. 3e).

Antifouling properties

Diamond is also the material with the highest atomic density and density (1.76×10^{23} at.cm^{-3} and 3.5 g.cm^{-3}, respectively). This results in chemical species diffusion being extremely limited within the diamond lattice. In other words, diamond contamination can occur only at the surface, which makes it easier to clean compared to other materials.

Moreover, boron-doped diamond (BDD) offers outstanding electrochemical properties [17] and, more specifically, a large potential window > 3 V in aqueous environments, enabling the production of highly oxidant radicals such as OH*, able to clean diamond electrodes. Several methods have been proposed to exploit the electrochemical antifouling properties of diamond surfaces, such as cathodic treatment [18], continuous anodic treatment [19–21], scanning potential methods [22], or pulsed current methods [23, 24]. Recently, this last method has been demonstrated to enable antifouling properties against oils [24].

Optical windows may be exposed to different kinds of contamination in outdoor operation. To provide an antifouling property to structured windows, a coating of ~ 100 nm of BDD, with a doping level inducing low absorption in IR (~ 10^{18} at.cm^{-3}), has been deposited on a nanostructured window. To analyze the electrochemical cleaning process, we monitored by SEM a silicon nanostructured window coated by BDD and previously contaminated in a mix of oil/gasoline. Images of Fig. 4 illustrate the surface quality of the structures during the cleaning process. In Fig. 4a, the structures are completely covered by oil and gazoline. In Fig. 4b, the electrochemical processing starts by applying a low current of ~ 100 mA on the 1 cm^2 sample. In Fig. 4c, the mixture has already started to be removed partially. In Fig. 4d, the contamination is completely removed after few minutes of activation, hence demonstrating the efficiency of the electrochemical cleaning processed with an anodic treatment with a continuous current of 100 mA/cm^2 for a few minutes, and the resilience of the window.

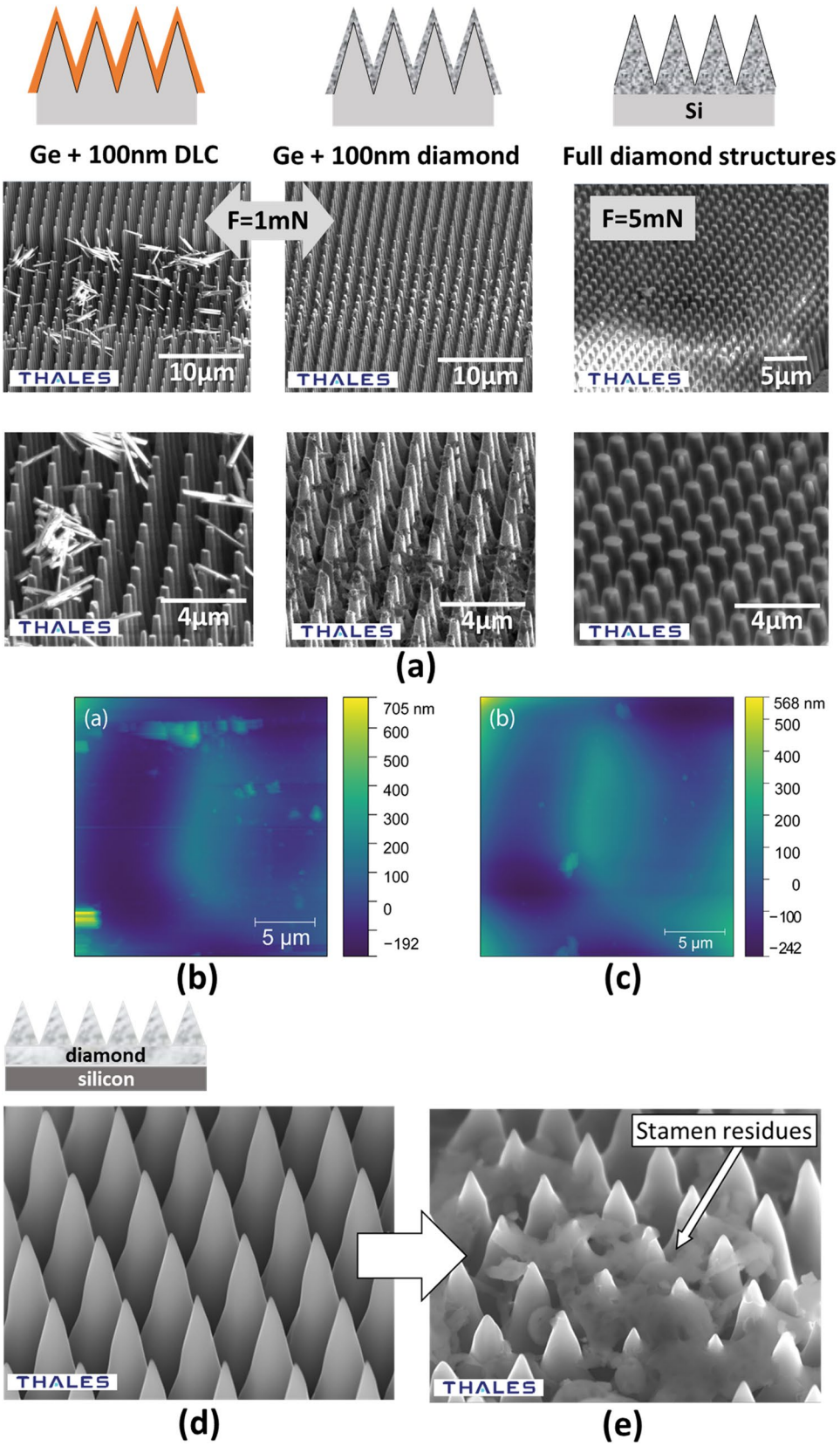

Fig. 3 **a** Comparison of failure mechanisms for nanostructured samples through SEM analysis. Background deconvoluted (spherical fit) AFM scan of the indenter tip before (**b**) and after (**c**) nanoscratch testing. SEM before (**d**) and after (**e**) abrasion tests of diamond microstructures (period ~ 1.5 µm) on silicon substrate

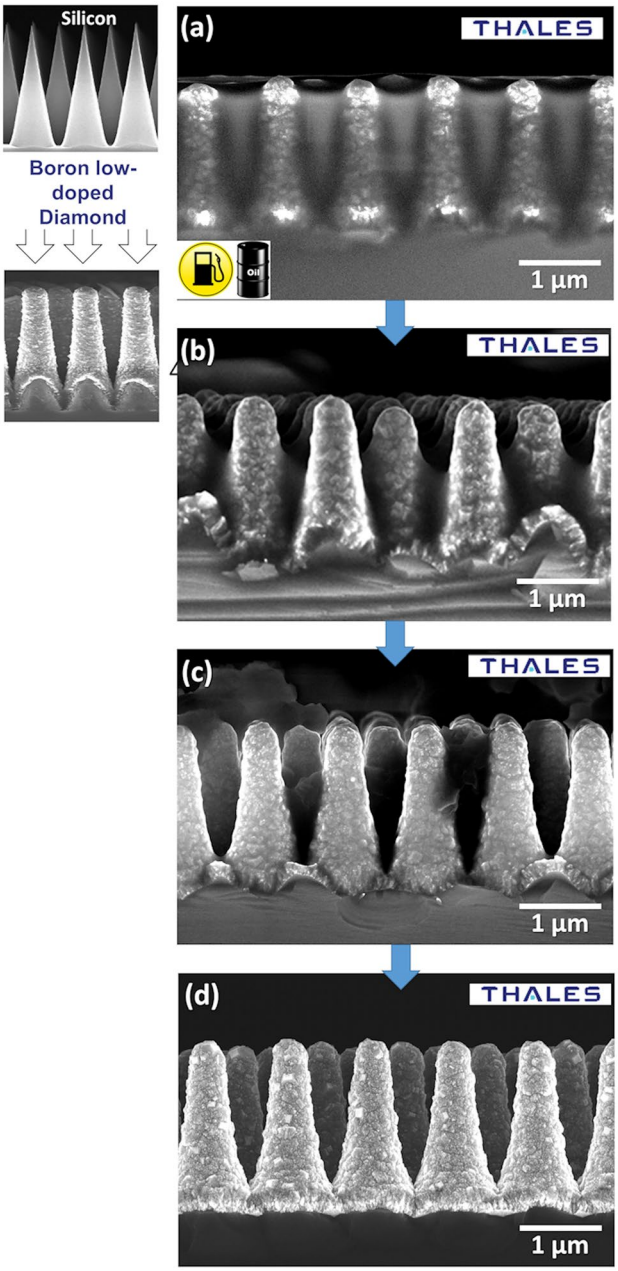

Fig. 4 SEM images of doped diamond-coated microstructured silicon window during the electrochemical activation. **a** The structured are completely drowned in oil and gasoline. **b**, **c** Activation of the electrochemical cleaning **d** The structures are cleaned of contaminants

Conclusion

In this paper, we demonstrated a nano-imprint-based process, combined with a plasma etching step, to microstructure and functionalize CVD diamond. This technology, which is compatible with large and curved surfaces, enables large-scale manufacturing compatible with optical surfaces. By taking advantage of diamond hardness and electrochemical properties, new windows enabling multi-physical properties convenient for imaging applications were demonstrated.

These multifunctional windows offer:

- antireflective properties (T > 80–90% for the whole window) over LWIR range,
- superhydrophic property with contact angle > 150°
- antirain and antimist properties
- enhanced mechanical resistance assessed by nanoscratch testing and showing the application of vertical forces up to 5mN without any breakage,
- antifouling properties able to have the window cleaned within a few minutes upon application of a small current of typ. 100 mA/cm^2.

Multifunctional diamond window tested on a LWIR camera has demonstrated its ability to ensure the imaging system's "clear" image even in a visually degraded environment (rain, mist…) or under harsh environmental conditions (chemical contamination, physical erosion…).

Acknowledgments The authors would like to thank the Agence de l'Innovation de Défense for partial support within the framework of the ASTRID project D-FACTO (grant agreement D-FACTO ANR-21-ASTR-0005). Nanoscratch measurements were carried out within the project NanoMECommons, funded by the EU H2020 Research and Innovation Action (Grant Agreement 952869).

Author contributions Raphaël Guillemet, Ph.D., was in charge and supervised the overall activities regarding multifunctional CVD diamond windows. Mane-Si Laure Lee, Ph.D., performed the structures design and optical simulations. Doriane Jussey was in charge of nano-imprint lithography and nanostructuration of the diamond windows. Emmanuel Scorsone, Ph.D., provided his long expertise concerning the synthetic diamond and its electrochemistry and was in charge, with Sirine Ben Khemis, Ph.D., of the diamond growth on the different substrates. Elyess Traouli worked on the windows electrocleaning setup. Edoardo Rossi, Ph.D., Saqib Rashid, Ph.D., and Prof. Marco Sebastiani were in charge of the mechanical tests on nanostructures through their unique platform of nanoindentation. Patrick Garabédian, Ph.D., Mane-Si Laure Lee, Ph.D., and Brigitte Loiseaux were in charge of the overall orientation of the work.

Funding This work has been partially funded under the framework of the ASTRID project D-FACTO (Grant Agreement D-FACTO ANR-21-ASTR-0005) and the EU H2020 Research and Innovation Action NanoMECommons (Grant Agreement 952869).

Data availability The authors can confirm that all relevant data are included in the article.

Declarations

Conflict of interests On behalf of all authors, the corresponding author states that there is no conflict of interest.

References

1. K. Park, H.J. Choi, C. Chang, R.E. Cohen, G.H. McKinley, G. Barbastathis, Nanotextured silica surfaces with robust superhydrophobicity and omnidirectional broadband supertransmissivity. ACS Nano **6**(5), 3789–3799 (2012). https://doi.org/10.1021/nn301112t
2. D. Infante, K.W. Koch, P. Mazumder, L. Tian, A.C. Carrilero, D. Tulli, D.E. Baker, V. Pruneri, Durable, superhydrophobic, antireflection, and low haze glass surfaces using scalable metal dewetting nanostructuring. Nano Res. **6**, p429-440 (2013). https://doi.org/10.1007/s12274-013-0320-z
3. D.A. Boyd, J.A. Frantz, S.S. Bayya, L.E. Busse, W. Kim, I.D. Aggarwal, M.K. Poutous, J.S. Sanghera, Modification of nanostructured fused silica for use as superhydrophobic, IR-transmissive, anti-reflective surfaces. Opt. Mater. **54**, 195–199 (2016). https://doi.org/10.1016/j.optmat.2016.02.035
4. D.A. Boyd, J.A. Frantz, R. Nimalan, L.E. Busse, W. Kim, S.S. Bayya, J.S. Sanghera, Periodically patterned germanium surfaces modified to form superhydrophobic, IR transmissive substrates. Opt Mater Exp. **6**, 3254–3261 (2016). https://doi.org/10.1364/OME.6.003254
5. R. Guillemet, M.S.L. Lee, J. Cholet, D. Jussey, A. Delboulbé, S. Xavier, B. Loiseaux, P. Garabédian, Nanoimprint-based subwavelength multifunctional optical windows: from visible to longwave infrared applications. Proc. SPIE **12274**, 122740Z (2022). https://doi.org/10.1117/12.2636213
6. M.S.L. Lee, R. Guillemet, A. Delboulbé, D. Jussey, J. Cholet, C. Arnoux, A. Banyasz, F. Hilbert, C. Monnereau, P. Baldeck, B. Loiseaux, P. Garabédian, P. Romero, Imaging enhancement using multifunctional subwavelength structured windows. Proc. SPIE **12274**, 122740G (2022). https://doi.org/10.1117/12.2636219
7. T. Mouterde, G. Lehoucq, S. Xavier, A. Checco, C.T. Black, A. Rahman, T. Midavaine, C. Clanet, D. Quéré, Antifogging abilities of model nanotextures. Nat. Mater. **16**(6), 658–663 (2017). https://doi.org/10.1038/nmat4868
8. W. Stork, N. Streibl, H. Haidner, P. Kipfer, Artificial distributed-index media fabricated by zero-order gratings. Opt. Lett. **16**(24), 1921–1923 (1991). https://doi.org/10.1364/OL.16.001921
9. M. Karlsson, F. Nikolajeff, Diamond micro-optics: microlenses and antireflection structured surfaces for the infrared spectral region. Opt. Expr. **11**, 502–507 (2003). https://doi.org/10.1364/oe.11.000502
10. P. Forsberg, M. Karlsson, Inclined surfaces in diamond: broadband antireflective structures and coupling light through waveguides. Opt. Expr. **21**, 2693–2700 (2013). https://doi.org/10.1364/OE.21.002693
11. M. Kiss, S. Mi, G. Huszka, N. Quack, Diamond diffractive optics recent progress and perspectives. Adv. Opt. Technol. **10**(1), 19–30 (2021). https://doi.org/10.1515/aot-2020-0052
12. A.D. Manni, H.S. Small, S.M. Consoles, B.D. MacLeod, D.S. Hobbs, "Optical properties of RAR nano-textured diamond for commercial LWIR applications," Proc. SPIE 13116, Nanoengineering: Fabrication, Properties, Optics, Thin Films, and Devices XXI, 1311606 (4 October 2024). https://doi.org/10.1117/12.3028539
13. M. Martínez-Calderon, J.J. Azkona, N. Casquero, A. Rodríguez, M. Domke, M. Gómez-Aranzadi, S.M. Olaizola, E. Granados, Tailoring diamond's optical properties via direct femtosecond laser nanostructuring. Sci. Rep. **8**, 14262 (2018). https://doi.org/10.1038/s41598-018-32520-0
14. A.B. Harker, J.F. DeNatale, "Diamond gradient index "moth-eye" antireflection surfaces for LWIR windows," Proc. SPIE 1760, Window and Dome Technologies and Materials III, (1992). https://doi.org/10.1117/12.130803
15. D.S. Hobbs, "Study of the environmental and optical durability of AR microstructures in sapphire, ALON, and diamond," Proc. SPIE 7302, Window and Dome Technologies and Materials XI, 73020J (2009). https://doi.org/10.1117/12.818335
16. V. Doquet, A. Tanguy, S. Hallais, R. Guillemet, J. Cholet, D. Jussey, Mechanical behavior of surface-patterned and coated Si or Ge wafers for superhydrophobic and antireflective light transmitting windows". J. Mater. Sci. **57**, 955–971 (2022). https://doi.org/10.1007/s10853-021-06794-1
17. A. Fujishima, Y. Einaga, T.N. Rao, D.A. Trykal., (2005). Diamond Electrochemistry ,Eds., Tokyo: BKC; Amsterdam: Elsevier, 2005, 546 + XXII. Russ J Electrochem 41, 1250–1251 https://doi.org/10.1007/s11175-005-0211-z
18. G.R. Salazar-Banda, A.E. de Carvalho, L.S. Andrade, R.C. Rocha-Filho, L.A. Avaca, On the activation and physical degradation of boron-doped diamond surfaces brought on by cathodic pretreatments. J. Appl. Electrochem. **40**, 1817–1827 (2010). https://doi.org/10.1007/s10800-010-0139-1
19. A. Kraft, Doped diamond: a compact review on a new, versatile electrode material. Int. J. Electrochem. Sci. **2**, 355 (2007). https://doi.org/10.1016/S1452-3981(23)17080-5
20. F. Beck, W. Kaiser, H. Krohn, Boron doped diamond (BDD)-layers on titanium substrates as electrodes in applied electrochemistry. Electrochim. Acta **45**, 4691 (2000). https://doi.org/10.1016/S0013-4686(00)00621-6
21. J.K. Holt, H.G. Park, Y. Wang, M. Stadermann, A.B. Artyukhin, C.P. Grigoropoulos, A. Noy, O. Bakajin, Fast mass transport through Sub-2-nanometer carbon nanotubes. Science **312**, 1034–1037 (2006). https://doi.org/10.1126/science.1126298
22. E. Vanhove, J. de Sanoit, J.C. Arnault, S. Saada, C. Mer, P. Mailley, P. Bergonzo, M. Nesladek, Stability of H-terminated BDD electrodes: an insight into the influence of the surface preparation. Phys. stat. sol. (a) **204**, 2931–2939 (2007). https://doi.org/10.1002/pssa.200776340
23. E. Mahe, D. Devilliers, Ch. Comninellis, Electrochemical reactivity at graphitic micro-domains on polycrystalline boron doped diamond thin-films electrodes. Electrochim. Acta **50**, 2263 (2005). https://doi.org/10.1016/j.electacta.2004.10.060
24. R. Kiran, E. Scorsone, J. de Sanoit, J.C. Arnault, P. Mailley, P. Bergonzo, Boron doped diamond electrodes for direct measurement in biological fluids: an in situ regeneration approach. J. Electrochem. Soc. (2013). https://doi.org/10.1149/2.014302jes